Journal of Fluids and Structures (1999) **13,** 127–142
Article No.: jfls. 1998.0189
All articles available online at http://www.idealibrary.com.on IDEAL

STROUHAL NUMBERS OF FLOW-EXCITED ACOUSTIC RESONANCE OF CLOSED SIDE BRANCHES

S. Ziada

Department of Mechanical Engineering, McMaster University Hamilton, Ontario, Canada

AND

S. Shine

Department of Mechanical Engineering, University of Nairobi, Nairobi, Kenya

(Received 14 February 1997 and in revised form 2 September 1998)

Flow-excited acoustic resonances of piping systems containing closed side-branches are often encountered in engineering applications. They are excited by the unstable shear layer which separates the mean flow in the main pipe from the stagnant fluid in the branch. The object of this paper is to develop a design chart that can be used to predict the critical flow velocities in the main pipe at which acoustic resonances are initiated. Model tests were carried out on three different configurations of side-branches (single, tandem, and coaxial branches). For each of these pipe configurations, the effects of the diameter ratio, the distance from an upstream elbow and the acoustic damping are investigated in some detail. The test results are implemented into a design chart to predict the flow velocity at the onset of resonance as a function of the system operational and geometric parameters.

1. INTRODUCTION

Acoustic standing waves in closed side-branches are often excited by the flow in the main pipe. The excited modes are typically those consisting of an odd number of quarter wavelengths along the length of the branch. The pulsation amplitudes generated by this type of acoustic resonance can be several times higher than the dynamic head in the main pipe. This level is sufficiently high to cause severe noise and/or vibration problems. Flow-excited acoustic resonances of closed side branches have been reported in the literature for a wide variety of practical applications, including natural gas, steam and water piping systems. In power plants for example, a turbine by-pass pipe forms two closed side-branches when the by-pass valve is closed; one branch upstream of the valve is connected to the fresh steam pipe, and a downstream branch connected to the cold reheat pipe. Chen & Stürchler (1977) and Gillessen & Roller (1989) reported vibration problems in such pipe arrangements. Acoustic resonances may also occur in pipe branches leading to safety valves, to boiler relief valves, or to any auxiliary unit when the isolation valve is closed, see e.g. Baldwin & Simmons (1986) and Bernstein & Bloomfield (1989). Closed side-branches can also be found in pumping and compressor stations, in which standby units are normally separated from the system by means of isolation or check valves. Chen & Florjancic (1975) and Bruggeman (1987) reported serious pipe vibrations in pumping and compressor installations.

0889–9746/99/010127 + 16 $30.00

Acoustic resonances of side-branches are caused by a feedback excitation mechanism referred to in the literature as a "fluid-resonant mechanism" (Rockwell & Naudascher 1978; Stoneman *et al.* 1988; Ziada 1994). As shown in Figure 1, the feedback is provided by the acoustic particle velocity of the resonant standing wave in the side-branch. This particle velocity induces new perturbations in the unstable shear layer at the separation location. As the shear-layer perturbations are amplified and convected downstream, they interact with the acoustic field and produce acoustic energy which reinforces the resonance of the acoustic mode. Side-branches are particularly liable to resonance, because the particle velocity of the resonant modes has its maximum amplitude at the location of the shear layer. This makes the excitation of the shear layer by the resonant acoustic mode as well as the interaction of the resulting shear-layer oscillations with the resonant acoustic mode very efficient.

Most of the recent theoretical models of this excitation mechanism are based on the acoustic analogy developed by Howe (1975, 1980). He showed that the instantaneous acoustic power, $\mathscr{P}$, generated by vorticity, $\boldsymbol{\omega}$, convecting within a sound field is given by

$$\mathscr{P} = -\rho \int \boldsymbol{\omega} \cdot (\mathbf{v} \times \mathbf{u})\, \mathrm{d}\mathscr{V}, \tag{1}$$

where ρ is the fluid density, $\mathbf{v}$ is the fluid velocity, $\mathbf{u}$ the particle velocity of the sound field, and $\mathscr{V}$ is the volume containing the vorticity field. Thus, acoustic resonances will be self-sustained if the integral of the acoustic power over an acoustic cycle is positive, and this implies that a favourable timing of vorticity convection with respect to the sound cycle must be maintained.

By means of this acoustic analogy and flow visualization techniques, Bruggeman (1987), Stoneman *et al.* (1988), Graf (1989), Peters (1993), Ziada (1994) and others have shown that

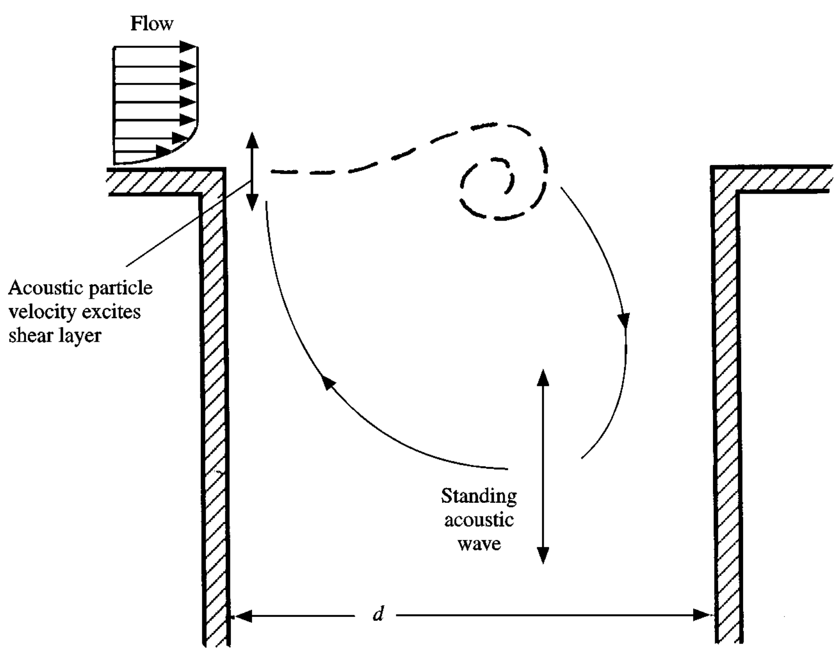

Figure 1. Feedback mechanism of flow-excited acoustic resonances of closed side-branches (the fluid-resonant mechanism).

resonances will be initiated when the convection velocity of the shear layer vortices reaches a favourable value such that a net acoustic energy is produced over a complete cycle. When the acoustic pulsation is small, which is the case at the onset of resonance, the convection velocity of the shear-layer oscillation is dependent on the "local" characteristics of the velocity profile at the branch mouth and consequently on the pipe geometry upstream of, and at the mouth of, the branch. The onset and the velocity range of resonance may be influenced also by the acoustic damping due to radiation, viscous and heat conduction losses in the associated piping system. The object of the present work is to investigate experimentally the effect of the above-mentioned parameters on the critical flow velocity (V_o) for the onset of resonance. The test results are then used to construct a simple design chart of critical Strouhal numbers (S_o) which reflects the effects of flow and geometrical parameters. The critical flow velocity in the main pipe can be estimated from the design value of S_o according to the formula

$$V_o = f_1 d/S_o, \tag{2}$$

where d is the side-branch diameter, and f_1 is the acoustic resonance frequency.

Figure 2 shows the three arrangements of side-branches that are tested in this study, together with schematic presentations of their lowest resonance modes and the patterns of the acoustic flux associated with these modes. Note that the distance between the tandem branches, ℓ, and the main pipe diameter, D, are much smaller than the wavelength of the acoustic modes.

In the single branch case, Figure 2(a), the pulsation amplitude in the branch is strongly influenced by the acoustic radiation into the main pipe, and consequently by the friction and heat conduction losses in the main pipe as well as by the radiation losses at the main pipe terminations. For example, Jungowski *et al.* (1989) have shown that increasing the diameter of the branch, d, with respect to that of the main pipe, D, which increases the radiation losses into the main pipe, is associated with a rapid reduction in the pulsation amplitude at resonance.

In the case of two branches, Figure 2(b, c), which are well tuned (i.e. of equal length) and in close proximity, i.e., $\ell \ll \lambda$, the acoustic flux at the mouth of one branch is equal but opposite to that at the mouth of the other branch. In the case of the coaxial branches for example, Graf & Ziada (1992) found that only 2% of the acoustic power in the branches is radiated into the main pipe. The two branches therefore strongly couple and form a subsystem with negligible radiation losses into the main pipe. Thus, the pulsation amplitude in the case of two (or multiple) branches can be drastically higher than that in the case of a single branch. Ziada & Bühlmann (1992) and Peters (1993) have shown that this is particularly the case for large values of d/D. Thus, the pipe geometries of Figure 2 were selected to allow the variation of radiation losses during the tests over a wide range: from a negligible value, as in the case of the coaxial branches, to a maximum value, as in the single branch case.

Viscous and heat conduction losses were varied during the tests by changing the diameter and the length of the side-branches, as well as by altering the static pressure during the tests.

The effect of the "local" mean velocity is investigated by adding an upstream elbow to distort the mean velocity profile at the mouth of the side-branches. The addition of the elbow also increases the flow turbulence at the branch mouth. However, earlier tests carried out by Ziada & Bühlmann (1992) have shown that increasing the turbulence level in the main pipe, by means of adding an orifice plate upstream of the tandem and coaxial branches, results in a substantial reduction in the pulsation amplitude, but a negligible effect on the critical flow velocity at the onset of resonance. In the present tests therefore, the alteration of the critical velocity resulting from the addition of the elbow is attributed to changes in the velocity profile rather than in the turbulence intensity.

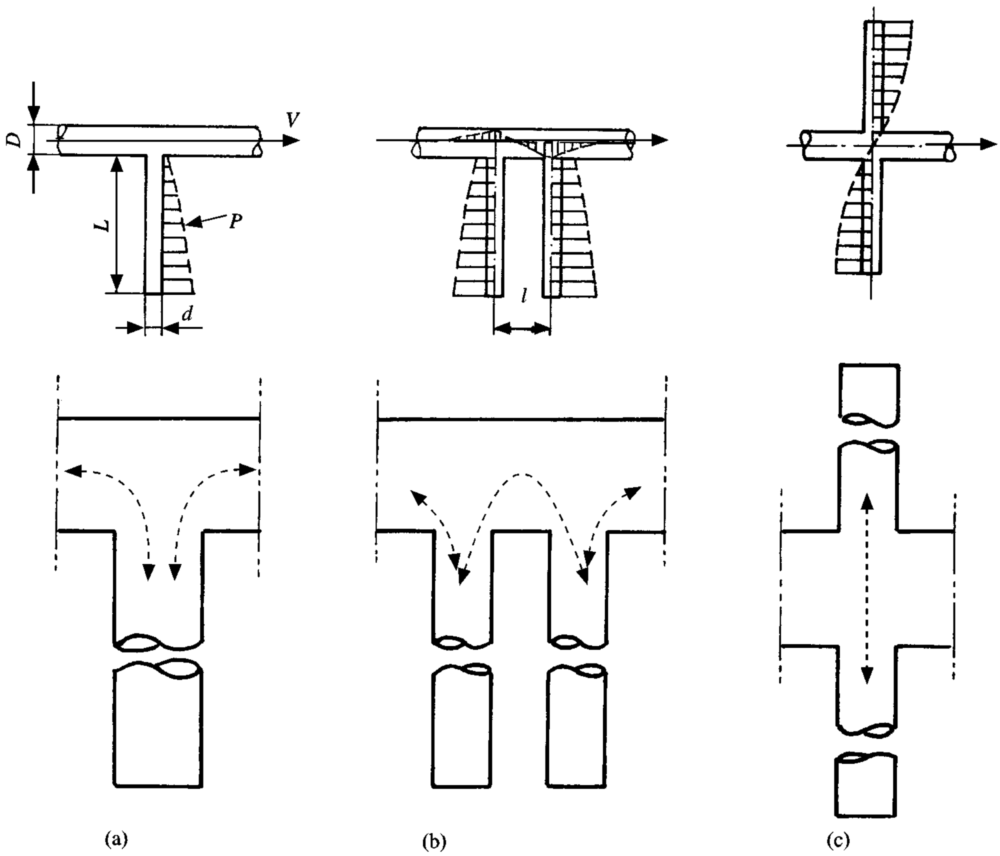

Figure 2. Tested arrangements of side-branches showing the acoustic pressure distribution of the first acoustic mode and the associated acoustic flux: (a) single branch; (b) tandem branches; (c) coaxial branches. The arrows in the bottom figures indicate the acoustic flux of the resonant acoustic modes.

2. EXPERIMENTAL FACILITY

A pressurised-air test facility was used to carry out the tests. As shown in Figure 3, the facility is equipped with a filter, a low-noise pressure regulator and an orifice plate to measure the flow rate. All pipes were made of steel and the T-joints of the branches had sharp edges. Two absorption silencers were installed at both ends of the test-section to make the main pipe less reactive and, therefore, reduce the influence of the main pipe acoustics on the acoustical response of the side-branches. It was possible to vary the static pressure (P_s) during the tests by means of a throttle valve, which was installed at the downstream end of the system.

The inner diameter of the main pipe was $D = 89$ mm. Three sets of side-branches with diameter ratios of $d/D = 0{\cdot}135, 0{\cdot}25$ and $0{\cdot}57$ were investigated. As shown in Figure 2, single tandem and coaxial side-branches were tested for each diameter ratio. The length of the branches (L) was also varied by means of pistons which could be moved inside the branches. However, the two pipes forming the tandem or the coaxial geometries were always of equal length.

The initial set-up included a straight piece of pipe, $25D$ length, upstream of the branches. Later on, a 90°-elbow with a radius of $3D$ was installed upstream (Figure 4) to investigate

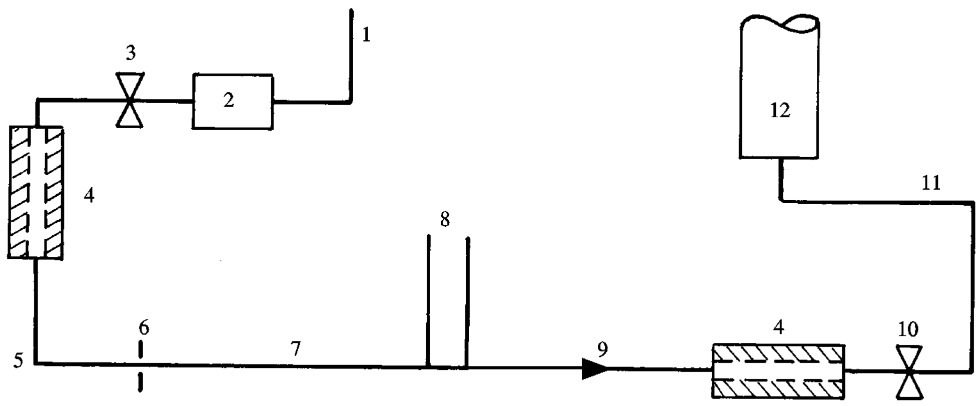

Figure 3. Schematic presentation of the test facility. The numbers denote: 1, pressurized air supply; 2, filter; 3, low-noise pressure regulator; 4, absorption silencer; 5, pipe (3·1 m); 6, metering orifice; 7, upstream pipe (5·05 m); 8, side branches; 9, downstream pipe (1·7 m); 10, throttle valve; 11, high pressure hose; 12, exhaust chimney.

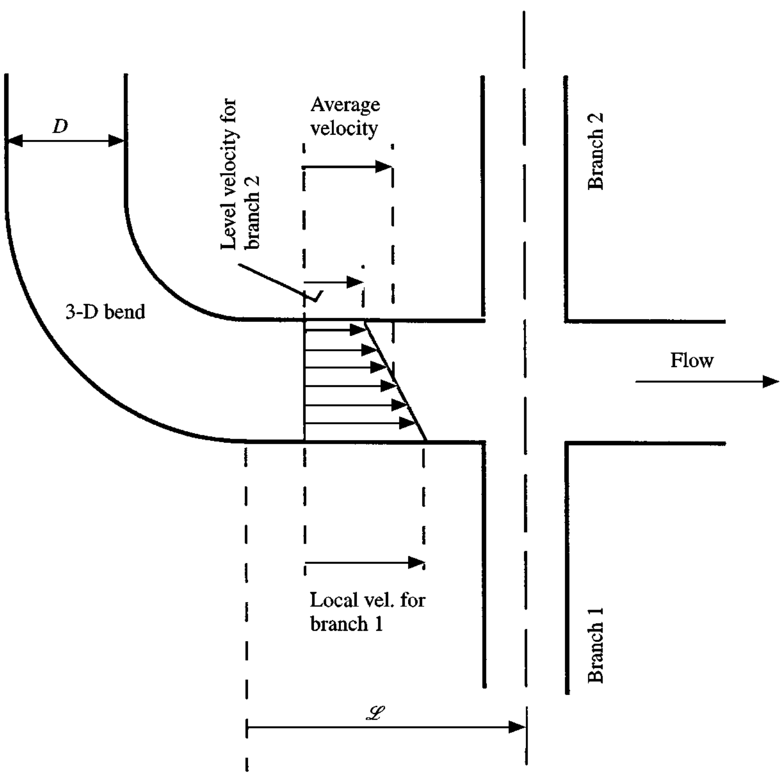

Figure 4. Schematic presentation of a nonuniform velocity profile (due to an upstream elbow) approaching two side-branches. Note that for the purposes of simplicity, a linear profile is shown.

the effect of the mean velocity profile on the onset of resonance. The side-branch(es) and the elbow were always in the same plane and the distance between them ($\mathscr{L}$) was varied. In most of the tests, the branches were positioned at the outer side of the elbow, i.e. similar to branch 1 in Figure 4.

The mean velocity (V) in the main pipe was calculated from the flow rate that was measured by means of the orifice plate. The pressure fluctuations at the closed ends of the branches were measured with the aid of Kistler transducers. A dual channel spectrum analyser was used to analyse the pressure signals.

The maximum flow velocity in the main pipe was limited by the maximum capacity of the facility (2 000 m^3/hr) and the test pressure. A maximum Reynolds number of $0{\cdot}5 \times 10^6$ was reached during tests, but that at the onset of resonance was less than $0{\cdot}26 \times 10^6$. These values are comparable to those encountered in many practical applications.

The flow velocity at the onset of resonance is defined in this paper as the velocity at which the slope of the acoustic response curve changes abruptly.

3. EFFECT OF RADIATION AND VISCOUS LOSSES

The objective of this section is to study the effect of acoustic damping on the onset of acoustic resonances of side-branches. To achieve this, the diameter ratio d/D was kept constant, whereas the radiation, viscous and heat conduction losses of the side-branches were varied. Radiation losses into the main pipe can be varied by altering the arrangement of the side-branches. As mentioned earlier, the coaxial branches have the lowest whereas the single branch has the highest radiation losses.

Acoustic damping in the side-branch due to viscous and heat conduction losses depends on the acoustic attenuation constant, α, which is given by

$$\alpha = [\mu_e f/4\pi\rho]^{1/2}/dC \quad \text{(Nepers/m)}, \tag{3}$$

where μ_e is the equivalent coefficient of viscosity which includes the effect of heat conduction, C is the speed of sound, d is the branch diameter, and f is the oscillation frequency; for more details, see Kinsler & Frey (1950). The acoustic attenuation can therefore be decreased by increasing the static pressure P_s to increase the fluid density, or by reducing the length of the side-branch. It should be noted, however, that a reduction in the side-branch length (L) increases the resonance frequency ($f \approx C/4L$) and therefore α becomes higher proportionally to $1/\sqrt{L}$, whereas the total attenuation loss (αL) decreases proportionally to L. Thus, the net effect of shortening the branch is a reduction in viscous and heat conduction losses.

Figure 5 shows a comparison between the acoustic responses of two tandem and two coaxial branches of similar diameter ratio ($d/D = 0{\cdot}57$). The amplitude of the acoustic pulsation, P, was measured at the closed end of the branch and is normalized by the dynamic head in the main pipe, $\frac{1}{2}\rho V^2$. The Strouhal number is defined by

$$S = f_1 d/V, \tag{4}$$

where f_1 is the frequency of the first acoustic mode (i.e., the one-quarter wavelength mode). *The Strouhal number becomes smaller as the flow velocity in the main pipe V is increased.* As expected, because of the difference in radiation losses, the coaxial branches have a larger resonance amplitude and a wider resonance (or lock-in) range than those of the tandem branches. However, the Strouhal number at the onset of resonance is virtually the same in both cases ($S_o \approx 0{\cdot}55$). Thus, the radiation losses seem to have a negligible effect on the *onset of resonance*.

The effect of viscous losses on the acoustic response of the coaxial arrangement is depicted in Figures 6 and 7. Both figures show the effect of increasing viscous losses (αL) by an amount equivalent to 50% of its original value, first by altering the test pressure, Figure 6, and then by increasing the length of the branch, Figure 7. The pulsation amplitude and the lock-in range increase as viscous losses are reduced. When the pulsation amplitude becomes sufficiently large, it exhibits hysteresis with the flow velocity. This non-linear

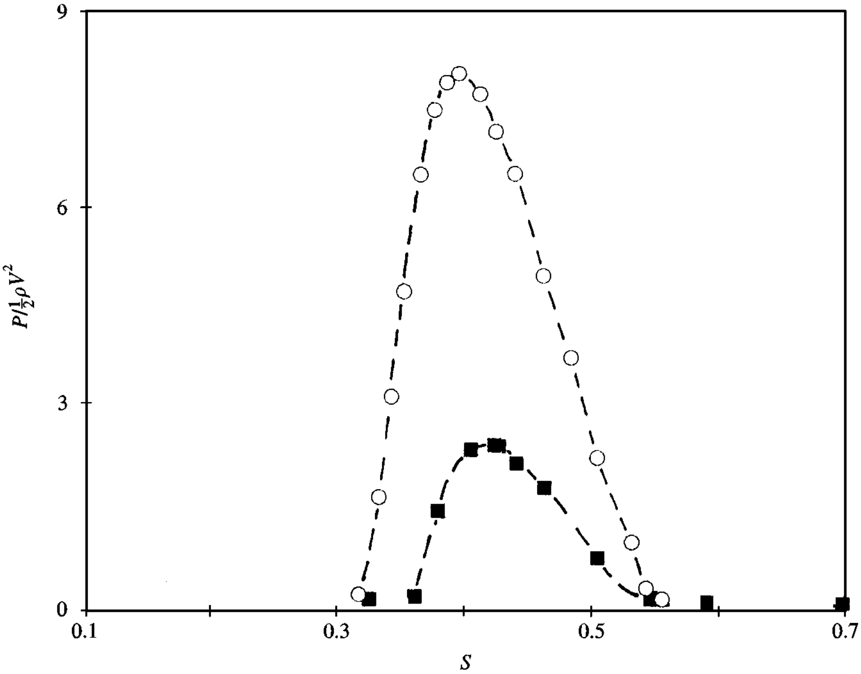

Figure 5. Amplitude of acoustic pulsation as a function of Strouhal number showing the effect of radiation damping. $d/D = 0{\cdot}57$, $P_s = 4$ bar; ○, coaxial branches, $L = 110{\cdot}5$ cm, $f_1 = 72{\cdot}5$ Hz; ■, tandem branches, $L = 100$ cm, $f_1 = 80$ Hz.

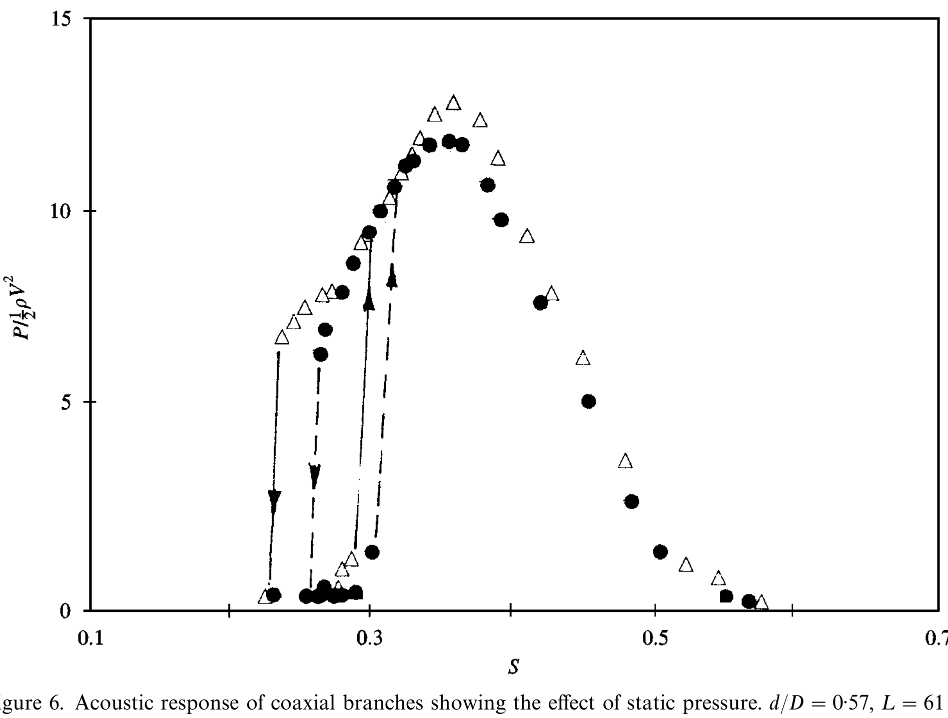

Figure 6. Acoustic response of coaxial branches showing the effect of static pressure. $d/D = 0{\cdot}57$, $L = 61$ cm, $f_1 = 132$ Hz; ●, $P_s = 1{\cdot}5$ bar; △, $P_s = 3{\cdot}5$ bar.

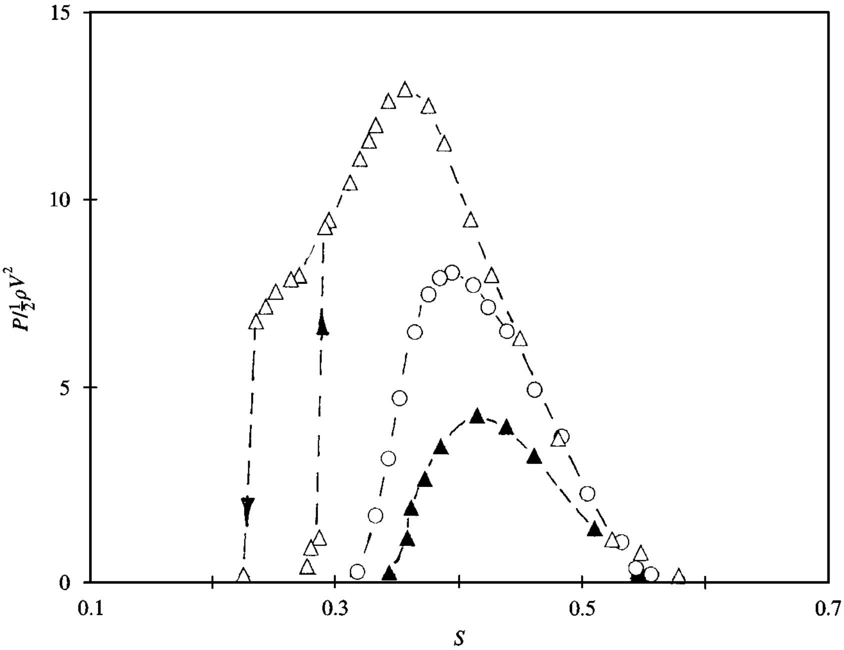

Figure 7. Acoustic response of the coaxial branches showing the effect of the branch length (i.e., the effect of acoustic attenuation). △, $L = 61$ cm, $f_1 = 132{\cdot}5$ Hz, $P_s = 3{\cdot}5$ bar; ○, $L = 110{\cdot}5$ cm, $f_1 = 72{\cdot}5$ Hz, $P_s = 4$ bar; ▲, $L = 158{\cdot}5$ cm, $f_1 = 50$ Hz, $P_s = 4$ bar.

feature has been investigated in some detail for the case of closed side-branches by Graf & Ziada (1993) and Ziada (1994).

Despite the large differences in the pulsation amplitude and the resonance range, the resonance starts in all the cases shown Figures 6 and 7 at the same value of Strouhal number ($S_o \approx 0{\cdot}55$). These results are in agreement with those published by Peters (1993) for coaxial side-branches with a diameter ratio of $d/D = 1$. Altering viscous losses in this pipe configuration by a factor of 8, by varying the length of the branches from 0·1 m to 0·397 m and the test pressure from 1 bar to 15 bar, influenced the pulsation amplitude and the lock-in range substantially, *but had a negligible effect on the Strouhal number at the onset of resonance.* Thus, it can be concluded that the effect of viscous and radiation losses on the Strouhal number at the onset of resonance is very small and can be neglected.

4. EFFECT OF THE DIAMETER RATIO

Figure 8 shows test results of single, tandem and coaxial branches for three different diameter ratios ($d/D = 0{\cdot}135$, 0·25 and 0·57). The maximum amplitude at resonance increases with the diameter ratio, especially for the coaxial case which produces the strongest resonance. In each case of diameter ratio, the resonances of the tandem and the coaxial branches start at similar Strouhal numbers. For the single-branch case, it is more difficult to determine the onset of resonance because the pulsation amplitude is rather small in general. In these cases, the response curves were blown up and the criterion of abrupt change in the slope was used to determine the onset of resonance. It is clear from Figure 8 that the resonance range, and in particular the onset of resonance, shifts to lower Strouhal numbers (i.e. to higher velocities) as the diameter ratio is decreased. This feature is delineated in

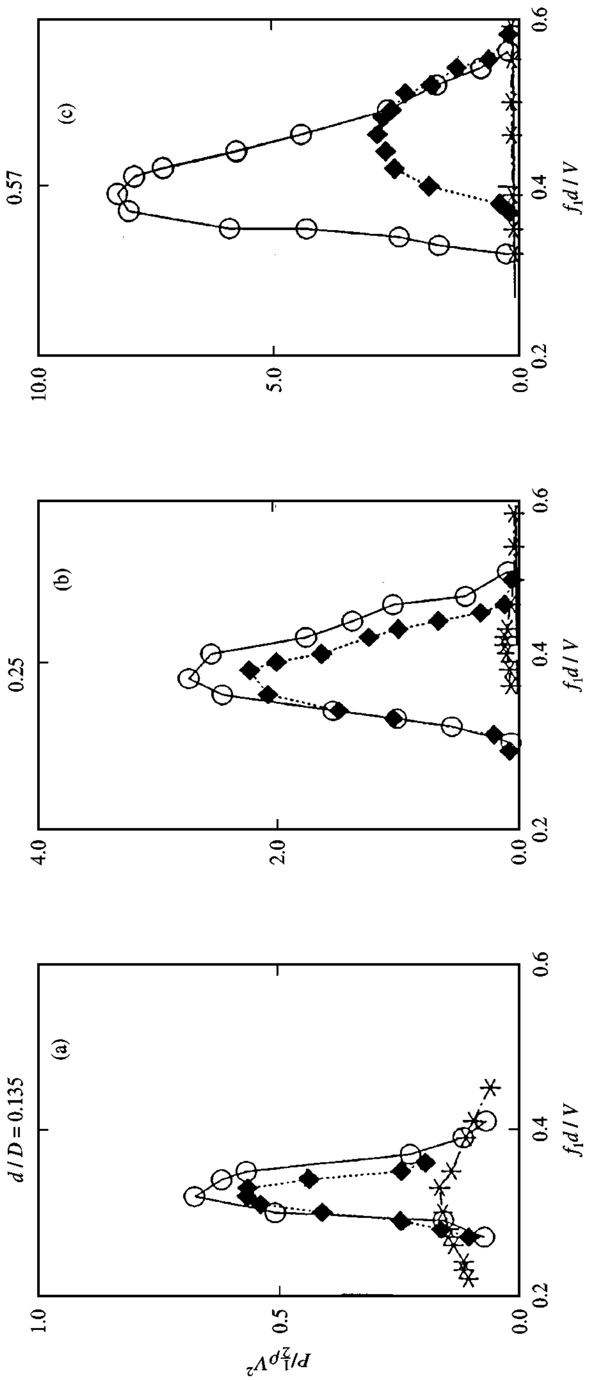

Figure 8. Comparison between the acoustic responses of single, tandem and coaxial side-branches for several values of diameter ratios: *, single; ◆, tandem; and ○, coaxial branches. (a) $d/D = 0{\cdot}135$; (b) $d/D = 0{\cdot}25$; (c) $d/D = 0{\cdot}57$.

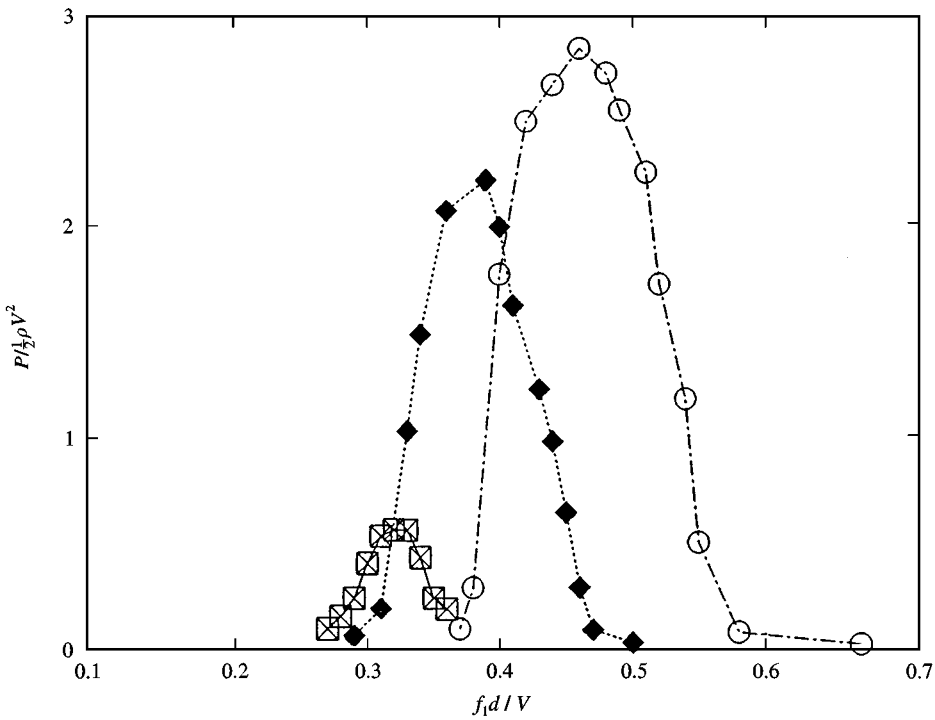

Figure 9. Effect of the diameter ratio of tandem branches on the critical Strouhal number of the onset of resonance. ■, $d/D = 0{\cdot}135$; ◆, 0·25; ○, 0·75.

Figure 9 which shows typical resonance curves of tandem branches with different diameter ratios. The critical Strouhal number S_o is reduced, i.e., the onset of resonance is delayed, when d/D is decreased. The effect of d/D on S_o is seen to be quite strong and should be taken into account when evaluating the liability of a system to resonance.

The relation between S_o and d/D stems from the alternation of the convection velocity of the vortices forming at the branch mouth when d/D is varied. This is because the size of the formed vortices scales with the diameter of the side-branch (Ziada 1994). Since the boundary-layer thickness in the main pipe is independent of the side-branch diameter, a larger size vortex will experience a higher mean velocity and will be swept faster along the branch mouth. The phase condition for the onset of oscillation, i.e., the favourable phasing between the vortex convection velocity and the acoustic oscillation, will therefore be achieved at a lower reduced velocity when the diameter of the side-branch (and consequently the vortex size) is larger.

5. EFFECT OF UPSTREAM ELBOWS

Resonances are initiated when the convection velocity of the shear-layer vortices is increased to an appropriate value such that a net positive acoustic energy is generated over a complete cycle. Thus, when the mean velocity profile in the main pipe is not uniform, one would expect the onset of oscillation to be related to the "local" flow velocity at the mouth of the branch, see Figure 4. In order to investigate this aspect, an elbow with a radius of $3D$ was installed upstream of the branch. The distance $\mathscr{L}$ between the elbow and the branch was varied from $1{\cdot}8D$ to $10D$. The effect of the upstream elbow was investigated for the cases of single, tandem and coaxial branches. However, neither the velocity profile nor the turbulence level at the outlet of the elbow were measured.

The acoustic response of a single side-branch ($d/D = 0{\cdot}135$) excited by a uniform flow ($\mathscr{L}/D = \infty$) is compared in Figure 10 with that excited by the (nonuniform) flow at the outlet of the elbow. The figure shows the results when the side-branch was installed first at the inner and then at the outer side of the elbow. The relative amplitude ($P/\frac{1}{2}\rho V^2$) and the Strouhal number are based on the average velocity calculated from the measured flow rate. The elbow is seen to affect the lock-in range and the amplitude of pulsation.

When the branch is at the outer side of the elbow, curve 1 in Figure 10, the local velocity is higher than the average velocity. The resonance therefore starts at a lower flow rate, i.e., at a higher S_o. Moreover, the relative amplitude becomes higher than the case of uniform flow (curve 3 in Figure 10). This increase, however, is rather superficial because the relative amplitude is based on the average velocity which is lower than the local velocity at the mouth of the branch, which excites the resonance. Conversely, when the branch is at the inner side of the elbow, curve 2 in Figure 10, the onset of resonance is delayed, i.e., it occurs at a higher flow rate, and the relative amplitude becomes (superficially) smaller. The three curves shown in Figure 10 may well become very close to each other if the local flow velocity is used to calculate the Strouhal number and the relative amplitude. This idea, however, has not been followed further, because its usefulness to practicing engineers is rather limited.

The effect of the elbow on the critical Strouhal number is weakened when the distance $\mathscr{L}/D$ between the elbow and the branch is increased. This feature is depicted in Figure 11, which shows measurements of a single branch with $d/D = 0{\cdot}25$ located at different distances from the upstream elbow. It is noteworthy that the effect of the elbow is still discernible, also when it is located at $10D$ upstream of the side-branch.

In the case of tandem branches also, the elbow promotes the onset of resonance and increases the relative amplitude of pulsation, Figure 12, whereas in the coaxial case, it has

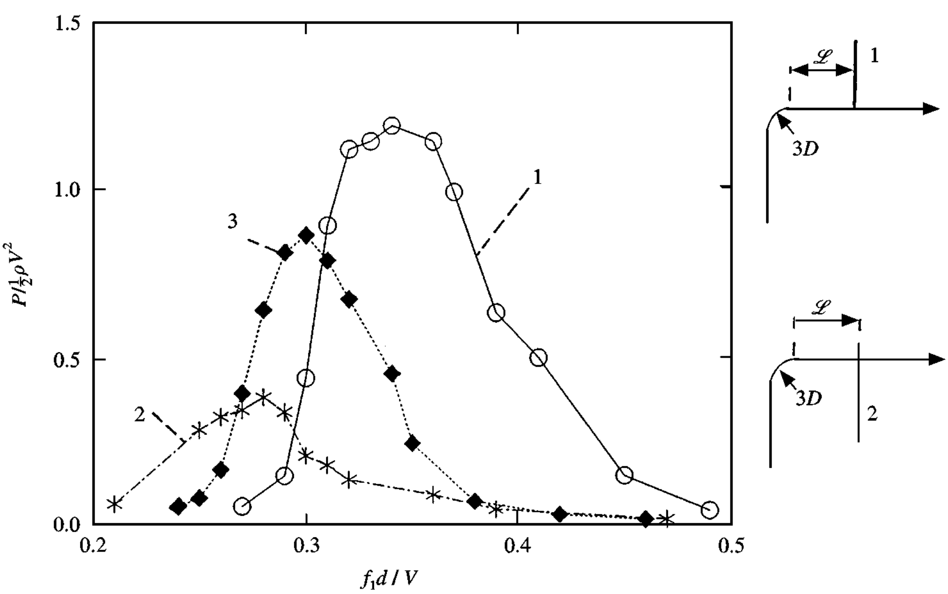

Figure 10. Effect of the upstream elbow on the acoustic response of a single branch; ○, branch at the outer side of the elbow; ∗, at the inner side; ◆, no elbow. $d/D = = 0{\cdot}135, f_1 = 490$ Hz, $\mathscr{L}/D = 1{\cdot}85$, $P_s = 3$ bar.

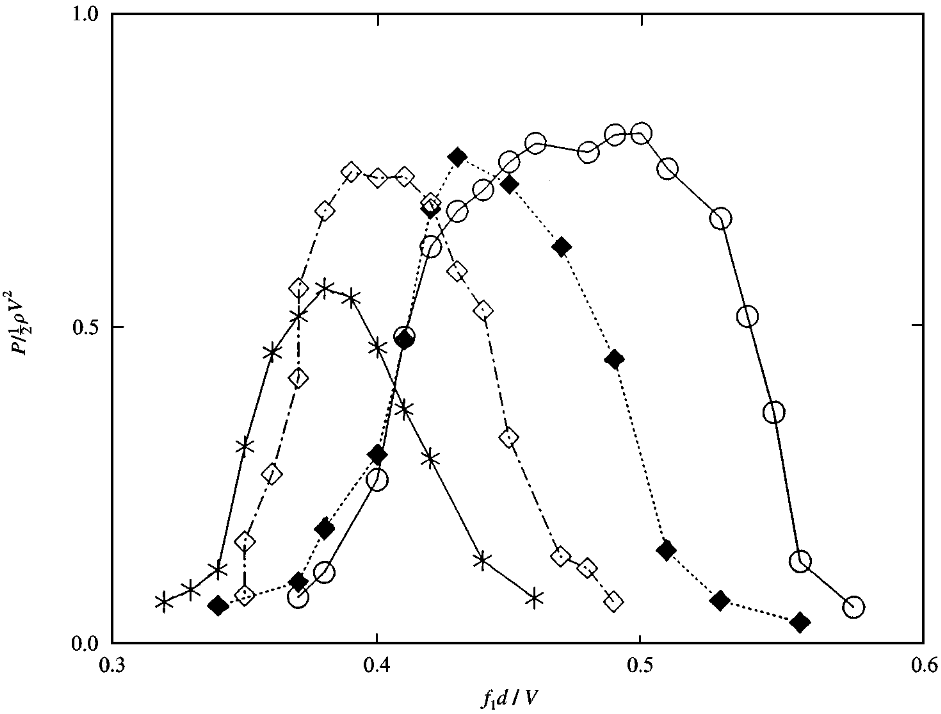

Figure 11. Pulsation amplitude versus Strouhal number for a single branch located at the outer side of, but at different distances ($\mathscr{L}$), from an upstream elbow; $d/D = 0{\cdot}25$, $f_1 = 326$ Hz, $P_s = 3$ bar. ○, $\mathscr{L}/D = 1{\cdot}8$; ◆, $\mathscr{L}/D = 6{\cdot}2$; ◇, $\mathscr{L}/D = 10$; ∗, $\mathscr{L}/D = \infty$.

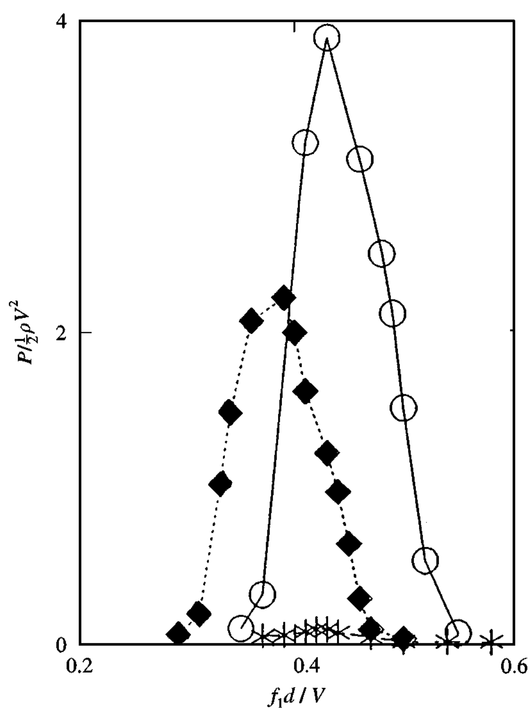

Figure 12. Effect of the upstream elbow on the resonance of two tandem branches installed at its outer side; $d/D = 0{\cdot}25$; ∗, single branch without elbow; ◆, tandem branches without elbow; ○, tandem branches with elbow at $\mathscr{L}/D = 3{\cdot}75$.

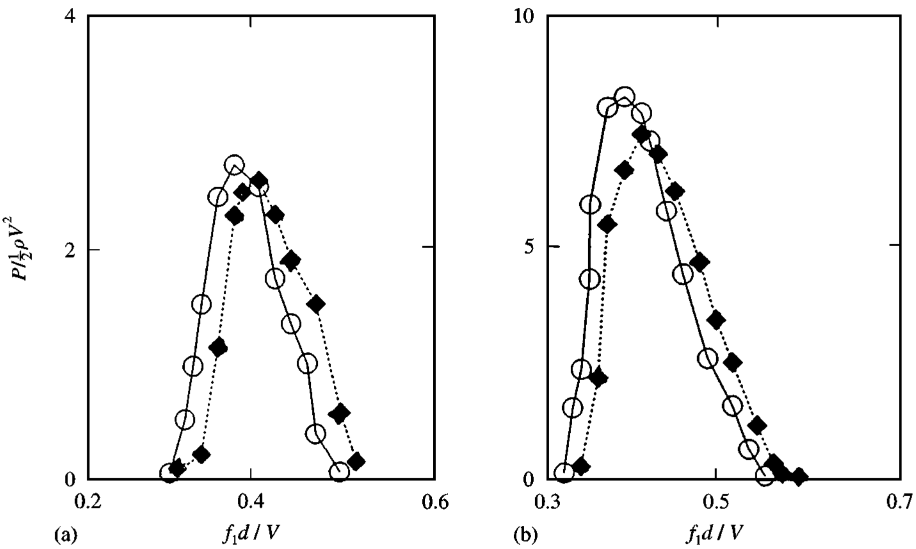

Figure 13. Effect of the upstream elbow on the resonance of two coaxial branches: ○, without elbow; ◆, with elbow at $\mathscr{L}/D = 3{\cdot}8$; (a) $d/D = 0{\cdot}25$; (b) $d/D = 0{\cdot}57$.

only a negligible effect, Figure 13. This difference seems to be due to the fact that the local flow velocities at the mouths of the two branches are similar, and higher than the mean velocity, in the tandem case, but different in the coaxial case. While the local velocity for one of the coaxial branches is higher than the average velocity, it is lower for the other branch, see Figure 4. The effect of this difference in local velocities seems to cancel itself out, resulting in only a slight difference from the case of uniform flow, Figure 13.

6. STROUHAL NUMBERS AT ONSET OF RESONANCE

It has been shown that the main parameters that influence the Strouhal number at the onset of resonance (S_o) are the diameter ratio d/D and the distance from an upstream elbow ($\mathscr{L}/D$), if there is any. Although the radiation and viscous losses strongly influence the maximum amplitude at resonance and the width of the lock-in range, they have been found to have a negligible effect on S_o. The Strouhal number data are therefore plotted as a function of the distance $\mathscr{L}/D$ in Figure 14, where the ratio d/D is taken as a parameter. It is seen that the value of S_o varies over a wide range ($0{\cdot}35 < S_o < 0{\cdot}62$). Thus, there is not a single value of S_o which is applicable for all diameter ratios, for example. In fact, the authors observed lower values of S_o in industrial applications with very small diameter ratios ($d/D < 0{\cdot}1$).

The increase in S_o as the diameter ratio is increased, which is depicted in Figure 14, agrees qualitatively with the findings of Jungowski *et al.* (1989). Although they did not report on the critical Strouhal numbers, they observed an increase in the Strouhal number at the maximum amplitude of resonance as the diameter ratio is increased.

The critical flow velocity (V_o) for the onset of resonance can be calculated from equation (1), where S_o is the value obtained from Figure 14. If the maximum flow velocity of the installation V_{max} is lower than V_o, resonance will not occur. Whenever V_o is found to be lower than V_{max}, design modifications should be adopted to make $V_{max} < V_o$. This can be achieved by enlarging the branch diameter at the junction or by shortening the branch

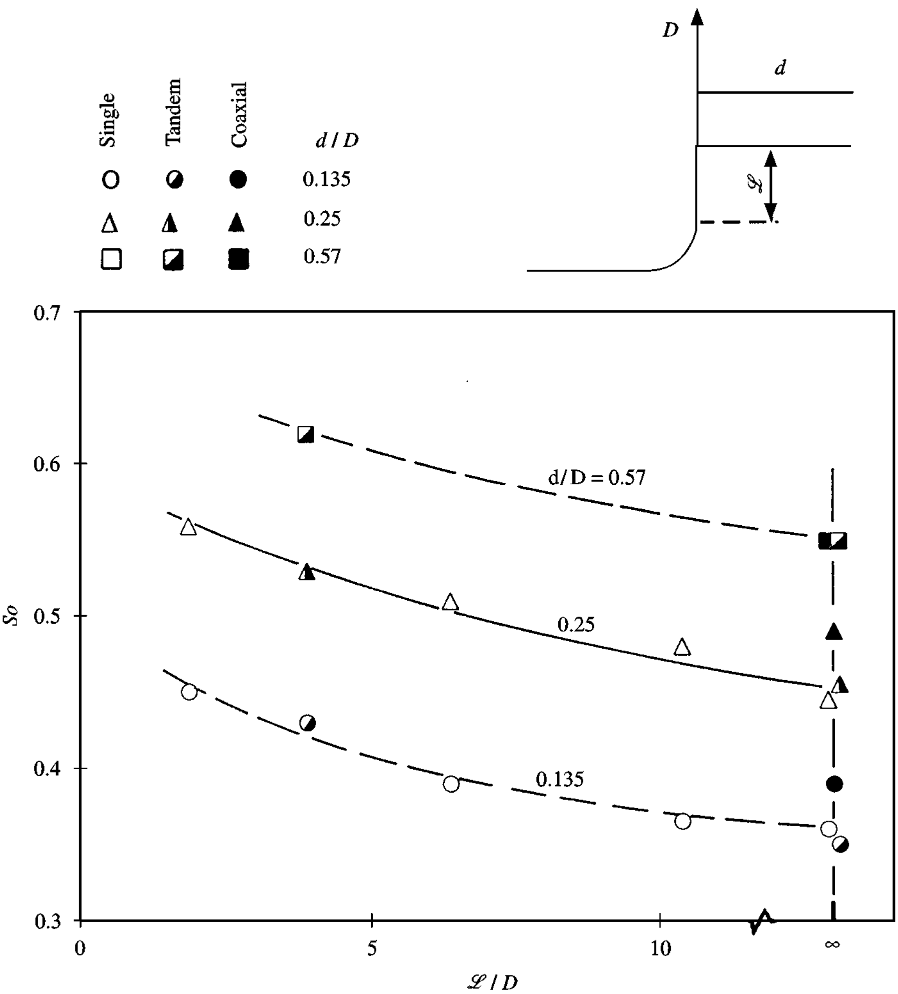

Figure 14. Design chart of critical Strouhal number at the onset of resonance (for proper use see comments in the text).

length to increase f_1. If these modifications are not possible, or they do not result in a sufficient increase in V_o, the pulsation amplitude at resonance should be estimated as outlined by Bruggeman (1987), Graf & Ziada (1992) or Peters (1993). The estimation of the pulsation amplitude indicates whether it is necessary, or not, to implement additional counter-measures such as those described by Ziada & Bühlmann (1992) and Ziada (1993).

Several remarks should be made here regarding the use of the Strouhal number chart given in Figure 14. First, when single or tandem branches are installed at the inner side of an upstream elbow, the critical Strouhal number is lower than that for $\mathscr{L}/D = \infty$, see curve 2 in Figure 10. In such cases, the use of a value corresponding to $\mathscr{L}/D = \infty$ is recommended because it results in conservative designs. Secondly, since the effect of upstream elbows on the critical Strouhal number of coaxial branches is negligible, a value corresponding to $\mathscr{L}/D = \infty$ should be used for coaxial branches, regardless of their position with respect to upstream elbows. Thirdly, it should be noted that Figure 14 is developed from the test results of one elbow radius. However, since this radius is relatively small ($3D$), the present results would be conservative for many practical applications which involve elbows with radius larger than $3D$. If the radius is smaller than $3D$, the designer should consider an additional margin of safety.

The developed chart can be used also for side-branches with square or rectangular cross-sections. However, the diameter d in the Strouhal number formula must be replaced by the equivalent diameter proposed by Bruggeman (1987),

$$d_e = (4/\pi)H, \tag{5}$$

where H is the width of the branch mouth in the flow direction.

When the corners of the branch mouth are rounded with a radius of curvature r, the critical flow velocity scales with $(d + r)$ instead of d (Bruggeman 1987). Figure 14, however, can still be used to estimate V_o by means of the formula

$$V_o = f_1(d + r)/S_o. \tag{6}$$

Finally, the value corresponding to $d/D = 0{\cdot}57$ can be used for larger diameter ratios. This suggestion is based on the fact that the Strouhal numbers reported by Peters (1993) for $d/D = 1$ are similar to the present results for $d/D = 0{\cdot}57$.

7. SUMMARY

Single, tandem and coaxial arrangements of closed side-branches have been tested to investigate the effects of the flow and design parameters on the critical Strouhal number at which acoustic resonances are *initiated*. The critical Strouhal number is found to be strongly influenced by the diameter ratio of the side-branch, relative to the main pipe diameter, and by the distance between the branch(es) and the nearest upstream elbow; i.e., by the shape of the velocity profile at the mouth of the branch. Although radiation and viscous losses strongly influence the maximum amplitude during resonance and the width of the lock-in range, they are found to have negligible effect on the Strouhal number at the onset of resonance. The test results are used to construct a design chart that can be used to predict the flow velocity in the main pipe at which side-branch resonances may be initiated.

References

Baldwin, R. M. & Simmons, H. R. 1986 Flow-induced vibration in safety relief valves. *ASME Journal of Pressure Vessel Technology* **108,** 267–272.

Bernstein, M. & Bloomfield, W. 1989 Malfunction of safety valves due to flow-induced vibrations. In *Flow-Induced Vibrations 1989* (eds M. K. Au-Yang, S. S. Chen, S. Kaneko & R. Chilukuri), PVP-Vol. 154, pp. 155–164. New York: ASME.

Bruggeman, J. C. 1987 Flow-induced pulsations in pipe systems. Doctoral Dissertation, Technische Universität Eindhoven, Eindhoven, The Netherlands.

Chen, Y. N. & Florjancic, D. 1975 Vortex-induced resonance in a pipe system due to branching. In *Proceedings of International Conference on Vibration and Noise in Pump, Fan and Compressor Installations*, pp. 79–86, University of Southampton, England.

Chen, Y. N. & Stürchler, R. 1977 Flow-induced vibrations and noise in a pipe system with blind branches due to coupling of vortex shedding. In *Internoise 77*, pp. B189–B203. Zürich.

Gillessen, R. & Roller, R. 1989 Verminderung und Besietigung von Schwingungen an Rohrleitungssystemen (Reduction and elimination of vibration of piping systems). In *Minderung von Rohrleitungsschwingungen*, VDI Berichte Vol. 748, pp. 195–222. Düsseldorf: VDI Verlag.

Graf, H. R. 1989 Experimental and computational investigation of the flow excited resonance in a deep cavity. Doctoral Dissertation, Department of Mechanical Engineering, Worcester Polytechnic Institute, U.S.A.

GRAF, H. R. & ZIADA, S. 1992 Flow-induced acoustic resonance in closed side branches: An experimental determination of the excitation source. In *Proceedings of ASME International Symposium on Flow-Induced Vibration and Noise, Vol. 7: Fundamental Aspects of Fluid-Structure Interactions* (eds M. P. Paidoussis, T. Akylas & P. B. Abraham), AMD-Vol. 51, pp. 63–80. New York: ASME.

HOWE, M. S. 1975 Contribution to the theory of aerodynamic sound, with application to excess jet noise and the theory of the flute. *Journal of Fluid Mechanics* **71,** 625–673.

HOWE, M. S. 1980 The dissipation of sound at an edge. *Journal of Sound and Vibration* **70,** 407–411.

JUNGOWSKI, W. M., BORTROS, K. K. & STUDZINSKI, W. 1989. Cylindrical side-branch as tone generator. *Journal of Sound and Vibration* **131,** 265–285.

KINSLER, L. E. & FREY, A. R. 1950 *Fundamentals of Acoustics*. New York: Wiley.

PETERS, M. C. A. M. 1993. Aeroacoustic sources in internal flows. Doctoral Dissertation, Technische Universität Eindhoven, Eindhoven, The Netherlands.

ROCKWELL, D. & NAUDASCHER, E. 1978 Review-self sustaining oscillations of flow past cavities. *ASME Journal of Fluids Engineering* **100,** 152–165.

STONEMAN, S. A. T., HOURGAN, K., STOKES, A. N. & WELSH, M. C. 1988 Resonant sound caused by flow past two plates in tandem in a duct. *Journal of Fluid Mechanics* **192,** 455–484.

ZIADA, S. 1993. Flow-excited resonances of piping systems containing side-branches: Excitation mechanism, counter-measures and design guidelines. *International Seminar on Acoustic Pulsations in Rotating Machinery*, pp. 1–34, AECL CANDU, Mississauga, Ontario, Canada.

ZIADA, S. 1994 A flow visualization study of flow-acoustic coupling at the mouth of a resonant side-branch, *Journal of Fluids and Structures* **8,** 391–416.

ZIADA, S. & BÜHLMANN, E. T. 1992 Self-excited resonances of two side-branches in close proximity. *Journal of Fluids and Structures* **6,** 583–601.

APPENDIX: NOMENCLATURE

d	side-branch diameter
D	main pipe diameter
f_1	frequency of the first $(\frac{1}{\lambda}\lambda)$ acoustic mode
L	length of side-branch
$\mathscr{L}$	distance between the side-branch and the upstream elbow
P	amplitude of acoustic pulsation
P_s	static pressure
S	Strouhal number ($S = fd/V$)
S_o	Strouhal number at onset of resonance ($S_o = f_1 d/V$)
V	mean velocity in main pipe
λ	wavelength of the first acoustic mode